

# Quasicrystal kirigami

Lucy Liu<sup>1†</sup>, Gary P. T. Choi<sup>2†</sup>, L. Mahadevan<sup>3,4\*</sup>

<sup>1</sup>Harvard College, Cambridge, MA, USA

<sup>2</sup>Department of Mathematics, Massachusetts Institute of Technology, Cambridge, MA, USA

<sup>3</sup>School of Engineering and Applied Sciences, Harvard University, Cambridge, MA, USA

<sup>4</sup>Departments of Physics, and Organismic and Evolutionary Biology, Harvard University, Cambridge, MA, USA

<sup>†</sup>These authors contributed equally to this work.

\*To whom correspondence should be addressed; E-mail: [lmahadev@g.harvard.edu](mailto:lmahadev@g.harvard.edu)

## Abstract

Kirigami, the art of introducing cuts in thin sheets to enable articulation and deployment, has till recently been the domain of artists. With the realization that these structures form a novel class of mechanical metamaterials, there is increasing interest in using periodic tiling patterns as the basis for the space of designs. Here, we show that aperiodic quasicrystals can also serve as the basis for designing deployable kirigami structures and analyze their geometrical, topological and mechanical properties. Our work explores the interplay between geometry, topology and mechanics for the design of aperiodic kirigami patterns, thereby enriching our understanding of the effectiveness of kirigami cuts in metamaterial design.

Kirigami is a traditional Japanese paper crafting art that has recently become popular among scientists and engineers. The simple idea of introducing cuts in a sheet of material has led to a surprisingly wide range of applications, including the design of super-stretchable materials [1], nanocomposites [2, 3], energy-storing devices [4] and robotics [5]. Numerous works have been devoted to the design of deployable kirigami patterns based on triangles [6], quads [7, 8] or even ancient Islamic tiling patterns [9], with recent efforts on generalizing their cut geometry [10–14] and cut topology [15, 16].

Almost without exception, these prior studies have manipulated the geometry, topology, and mechanics of tiling patterns with translational symmetry, most recently using periodic deployable

kirigami patterns based on wallpaper groups [17]. However, the crystallographic restriction theorem states that the order of the rotational symmetry in any periodic 2D patterns can only be 1, 2, 3, 4 or 6 [18]. This significantly limits the design space of periodic kirigami patterns. It is therefore natural to ask if kirigami might be possible using patterns that lack translational or rotational symmetry. *Quasicrystals* [19] and their tilings [20–25] are a natural class of aperiodic structures that fit this bill, with three representative examples being the Penrose tiling [26] (with 5-fold rotational symmetry), the Ammann–Beenker tiling [27] (with 8-fold rotational symmetry), and the Stampfli tiling [28] (with 12-fold rotational symmetry). Here we pose the problem of kirigami design from a new perspective: Is it possible to design radially deployable structures [29–32] based on quasicrystal patterns? We solve this problem by proposing three different design methods and analyzing their geometrical, topological and mechanical properties.

Our starting point is an aperiodic quasicrystal tiling pattern which we need to make deployable by choosing to cut it along appropriate edges to articulate the structure while keeping it as a single connected whole. Here we show that we can achieve deployability and also achieve *symmetry-preserving* patterns, with the special quasicrystal rotation orders preserved upon deployment in all three approaches. Moreover, we focus on the design of *rigid-deployable* quasicrystal patterns, in which all tiles do not undergo any bending or shearing throughout deployment.

A helpful way to think about a kirigami pattern’s structure is to consider its lattice representation, a graph where each tile is represented by a node. An edge between two nodes exists if their corresponding tiles are connected by a shared vertex around which both tiles can rotate freely. A pattern is rigidly deployable if it can be pulled apart along cuts so that tiles rotate away from each other and the pattern’s enclosed area increases without compromising tiles’ rigidity. As discussed in [17], 3-cycles in the lattice representation of a pattern cannot be rigidly deployed.

Consider three tiles lying so that any two tiles share an edge, like three regular hexagons that meet at a common vertex. If the tiles are connected in a 3-cycle, each pair of tiles must be

connected at one end of their shared edge. No two tiles are able to rotate away from each other and deploy. This is because both tiles are also connected to the third tile, which is rigid and cannot accommodate any deformation. However, if we have four or more tiles connected in a cycle, connections can be designed so that when two connected tiles rotate away from each other, the other tiles rotate as well to accommodate the deployment while still satisfying the system's constraints.

**The expansion tile method:** Our first approach to the design of deployable quasicrystal patterns aims to connect tiles so that the resulting lattice has no 3-cycles. One method is to make use of the expansion tiles introduced in [17], where thin tiles are added between existing tiles in the quasicrystal pattern. The new expansion tiles are connected to the tiles they are placed between, and they appear in the lattice representation as additional nodes in the middle of existing edges. The 3-cycles in the lattice structure are turned into 6-cycles instead, and hence the entire pattern becomes deployable. To illustrate this idea, we fabricate a physical model of a deployable 5-fold Penrose pattern obtained by this method (see Fig. 1(a) and SI Video S1), which consists of rigid cardstock paper tiles connected by threads (see SI Section S1 for more details). Note that the expansion tiles are not necessarily of the same width, and there may be gaps between the tiles in the pattern. To yield a closed and compact shape without gaps, one can consider ideal expansion tiles of infinitesimal width. Fig. 1(b)–(d) show the simulated deployments of three deployable quasicrystal patterns with ideal expansion tiles (see also SI Video S2–S4). It can be observed that the three patterns exhibit 5, 8 and 12-fold symmetry throughout deployment from a closed and compact contracted configuration to the fully deployed configuration, and a large size change is achieved. Here, the deployment simulations are performed using Python, with the 2D rigid body physics library Pymunk utilized. The deployment of each pattern is modeled by continually applying forces on the pattern's convex hull tiles, in the direction away from the pattern center (see SI Section S2 for more details). See SI Section S3.1 for more deployable

quasicrystal patterns produced by the expansion method.

**The tile removal method:** Our second approach for achieving deployability is to remove certain tiles in a given quasicrystal pattern, changing the lattice connectivity and introducing negative space. By taking a tile involved in each 3-cycle out of the pattern, we can again remove 3-cycles in the lattice and make the structure deployable. For instance, a deployable 5-fold Penrose pattern can be obtained by removing one type of rhombus tile in the tiling (Fig. 2(a)). Similarly, a deployable 8-fold Ammann–Beenker pattern can be obtained by removing all squares (Fig. 2(b)), and a deployable 12-fold Stampfli pattern can be obtained by removing all rhombi (Fig. 2(c)). Analogous to the expansion method, the deployable patterns produced by the tile removal method exhibit 5, 8 and 12-fold symmetry throughout deployment (see also SI Video S5–S7 and Section S3.2 for more results). Fig. 2(d) shows a physical model of a deployable Stampfli pattern (see also SI Video S8). We remark that while this method does not achieve a large size change because of the holes, it is useful for some applications as we can change the size and shape of the holes throughout deployment without changing the size of the entire structure much. For instance, one may design a flexible filter that allows some shapes to pass through at the initial state, and some other shapes to pass through at the deployed state.

**The Hamiltonian cycle method:** Our third method which does not require us to add or remove any tiles is based on manipulating the connectivity of the tiles. Furthermore, it is possible in edge to edge polygonal tilings to optimize expansion by connecting the tiles in a Hamiltonian cycle, which deploys into a single loop of connected tiles. We introduce the following graphic-theoretic approach to achieve this. Consider the lattice representation of a pattern, i.e. a graph  $G$  where the nodes are the tile centers and there exists an edge between two nodes if and only if the two corresponding tiles share a connected vertex [17]. By the Tutte theorem [33], every 4-connected planar graph has a Hamiltonian cycle (i.e. a closed loop that visits all nodes exactly once). For all three quasicrystal patterns we consider, note that each tile has at least three sides

and there are always some other tiles that share a common vertex with it, making the vertex degree  $\geq 4$  for all nodes in the associated graph  $G$ . Although  $G$  may not be planar (i.e. there may be edge crossings), one can always consider a subgraph  $\tilde{G}$  of  $G$  with a few edges connecting tiles in the same layer removed, thereby avoiding edge crossings while keeping the vertex degree  $\geq 4$ . Consequently, based on the 4-connected planar subgraph  $\tilde{G}$ , we can draw a Hamiltonian cycle and hence obtain a deployable structure with all tiles used (see SI Section S3.3 for more details). Fig. 3(a)–(c) show three examples of deployable Penrose, Ammann–Beenker and Stampfli patterns obtained by this method, in which a significant size change can be observed throughout the symmetry-preserving deployment (see SI Video S9–S11 and Section S3.3 for more results). A physical model of a deployable Ammann–Beenker pattern is shown in Fig. 3(d) (see also SI Video S12).

After establishing the three above design methods for producing deployable and symmetry-preserving quasicrystal patterns, it is natural to ask how the patterns produced by the three methods are different in terms of their geometrical, topological and mechanical properties. To quantify the geometrical change of each pattern under the deployment, we define the size change ratio of each deployable pattern by  $r_s = \frac{\text{Area of the fully deployed pattern}}{\text{Area of the contracted pattern}}$  and the perimeter change ratio by  $r_p = \frac{\text{Perimeter of the fully deployed pattern}}{\text{Perimeter of the contracted pattern}}$ . By evaluating  $r_s$  and  $r_p$  for various patterns, we observe that the Hamiltonian method achieves the largest  $r_s$  and  $r_p$  among the three design methods when the number of tiles  $n$  becomes sufficiently large (see SI Section S4.1 for the results). Moreover,  $r_s$  and  $r_p$  increase with  $n$  following the power law  $r_s \propto n$  and  $r_p \propto \sqrt{n}$  for the Hamiltonian method, which can be explained using a simple mathematical argument (see SI Section S4.1).

Next, we analyze the topology of the patterns by assessing the change in the number of holes of them (denoted as  $d_{\text{hole}}$ ) under deployment (see SI Section 4.2 for the results). We observe that the three design methods lead to significantly different topological behaviors. In particular,  $d_{\text{hole}}$  increases linearly with  $n$  with a slope of approximately 1/4 for the expansion method, while the

Hamiltonian method always gives  $d_{\text{hole}} = 1$  as it transforms a closed and compact pattern into a single loop throughout deployment (see SI Section 4.2 for more details).

Finally, we study the mechanics of the patterns by considering their infinitesimal rigidity [15, 34]. More specifically, we construct a rigidity matrix  $\mathbf{A}$  using the length and connectivity constraints given by each pattern, which allows us to determine the total internal degrees of freedom  $d_{\text{int}} = 2|\mathcal{V}| - \text{rank}(\mathbf{A}) - 3$ , where  $|\mathcal{V}|$  is the total number of vertices (see SI Section S4.3 for more details and the results). We observe that  $d_{\text{int}}$  increases approximately linearly with  $n$  for all three methods. In particular, the Hamiltonian method achieves the largest  $d_{\text{int}}$  among the three methods, with  $d_{\text{int}} \sim n$  (see SI Section S4.3 for more details).

We close with a brief consideration of the structure of the patterns during the process of deployment. It is well-known that the quasicrystal tilings are closely related to the Fourier transform of their diffraction pattern. While the deployable quasicrystal patterns produced by the three methods are symmetry-preserving throughout their deployment, their quasicrystalline order is not preserved. Indeed, one can observe a significant change in the Fourier transform at the beginning of the deployment process (see SI Section S5 for more details).

All together, we have uncovered a set of strategies for designing a deployable kirigami structure given any planar tiling pattern by adding tiles to it, removing tiles from it, or changing the connectivity of tiles in it. These approaches preserve some of the symmetries of the tilings and exhibit highly unusual geometrical, topological and mechanical features throughout deployment. Besides the 5-fold Penrose tiling, 8-fold Ammann–Beenker tiling and 12-fold Stampfli tiling considered in this work, the three design methods can also be applied to aperiodic tilings with other symmetry orders for achieving a large variety of symmetry-preserving deployable structures. Since the deployable structures produced by the three proposed design methods are significantly different from traditional kirigami structures in the sense that they are ordered but aperiodic throughout the entire deployment process, they naturally complement prior kirigami

approaches and may well pave the way for the design of novel deployable structures.

## References

- [1] Y. Tang and J. Yin, “Design of cut unit geometry in hierarchical kirigami-based auxetic metamaterials for high stretchability and compressibility,” *Extreme Mech. Lett.*, vol. 12, pp. 77–85, 2017.
- [2] M. K. Blees, A. W. Barnard, P. A. Rose, S. P. Roberts, K. L. McGill, P. Y. Huang, A. R. Ruyack, J. W. Kevek, B. Kobrin, D. A. Muller, *et al.*, “Graphene kirigami,” *Nature*, vol. 524, no. 7564, p. 204, 2015.
- [3] T. C. Shyu, P. F. Damasceno, P. M. Dodd, A. Lamoureux, L. Xu, M. Shlian, M. Shtein, S. C. Glotzer, and N. A. Kotov, “A kirigami approach to engineering elasticity in nanocomposites through patterned defects,” *Nat. Mater.*, vol. 14, no. 8, p. 785, 2015.
- [4] Z. Song, X. Wang, C. Lv, Y. An, M. Liang, T. Ma, D. He, Y.-J. Zheng, S.-Q. Huang, H. Yu, *et al.*, “Kirigami-based stretchable lithium-ion batteries,” *Sci. Rep.*, vol. 5, no. 1, pp. 1–9, 2015.
- [5] A. Rafsanjani, Y. Zhang, B. Liu, S. M. Rubinstein, and K. Bertoldi, “Kirigami skins make a simple soft actuator crawl,” *Sci. Robot.*, vol. 3, no. 15, p. eaar7555, 2018.
- [6] J. N. Grima and K. E. Evans, “Auxetic behavior from rotating triangles,” *J. Mater. Sci.*, vol. 41, no. 10, pp. 3193–3196, 2006.
- [7] J. N. Grima and K. E. Evans, “Auxetic behavior from rotating squares,” *J. Mater. Sci. Lett.*, vol. 19, no. 17, pp. 1563–1565, 2000.

- [8] D. Attard and J. N. Grima, “Auxetic behaviour from rotating rhombi,” *Phys. Status Solidi B*, vol. 245, no. 11, pp. 2395–2404, 2008.
- [9] A. Rafsanjani and D. Pasini, “Bistable auxetic mechanical metamaterials inspired by ancient geometric motifs,” *Extreme Mech. Lett.*, vol. 9, pp. 291–296, 2016.
- [10] M. Konaković, K. Crane, B. Deng, S. Bouaziz, D. Piker, and M. Pauly, “Beyond developable: computational design and fabrication with auxetic materials,” *ACM Trans. Graph.*, vol. 35, no. 4, pp. 1–11, 2016.
- [11] P. Celli, C. McMahan, B. Ramirez, A. Bauhofer, C. Naify, D. Hofmann, B. Audoly, and C. Daraio, “Shape-morphing architected sheets with non-periodic cut patterns,” *Soft Matter*, vol. 14, no. 48, pp. 9744–9749, 2018.
- [12] M. Konaković-Luković, J. Panetta, K. Crane, and M. Pauly, “Rapid deployment of curved surfaces via programmable auxetics,” *ACM Trans. Graph.*, vol. 37, no. 4, pp. 1–13, 2018.
- [13] G. P. T. Choi, L. H. Dudte, and L. Mahadevan, “Programming shape using kirigami tessellations,” *Nat. Mater.*, vol. 18, no. 9, pp. 999–1004, 2019.
- [14] G. P. T. Choi, L. H. Dudte, and L. Mahadevan, “Compact reconfigurable kirigami,” *Preprint, arXiv:2012.09241*, 2020.
- [15] S. Chen, G. P. T. Choi, and L. Mahadevan, “Deterministic and stochastic control of kirigami topology,” *Proc. Natl. Acad. Sci.*, vol. 117, no. 9, pp. 4511–4517, 2020.
- [16] G. P. T. Choi, S. Chen, and L. Mahadevan, “Control of connectivity and rigidity in prismatic assemblies,” *Proc. R. Soc. A*, vol. 476, no. 2244, p. 20200485, 2020.
- [17] L. Liu, G. P. T. Choi, and L. Mahadevan, “Wallpaper group kirigami,” *Preprint, arXiv:2102.10754*, 2021.

- [18] B. Grünbaum and G. C. Shephard, *Tilings and patterns*. WH Freeman & Co., 1986.
- [19] D. Shechtman, I. Blech, D. Gratias, and J. W. Cahn, “Metallic phase with long-range orientational order and no translational symmetry,” *Phys. Rev. Lett.*, vol. 53, no. 20, p. 1951, 1984.
- [20] N. Wang, H. Chen, and K. Kuo, “Two-dimensional quasicrystal with eightfold rotational symmetry,” *Phys. Rev. Lett.*, vol. 59, no. 9, p. 1010, 1987.
- [21] J. E. S. Socolar, “Simple octagonal and dodecagonal quasicrystals,” *Phys. Rev. B*, vol. 39, no. 15, p. 10519, 1989.
- [22] M. Baake and D. Joseph, “Ideal and defective vertex configurations in the planar octagonal quasilattice,” *Phys. Rev. B*, vol. 42, no. 13, p. 8091, 1990.
- [23] M. Baake, S. I. Ben-Abraham, R. Klitzing, P. Kramer, and M. Schlottman, “Classification of local configurations in quasicrystals,” *Acta Cryst. A*, vol. 50, no. 5, pp. 553–566, 1994.
- [24] M. Senechal, *Quasicrystals and geometry*. Cambridge University Press, 1996.
- [25] Y. Nagaoka, H. Zhu, D. Eggert, and O. Chen, “Single-component quasicrystalline nanocrystal superlattices through flexible polygon tiling rule,” *Science*, vol. 362, no. 6421, pp. 1396–1400, 2018.
- [26] R. Penrose, “The role of aesthetics in pure and applied mathematical research,” *Bull. Inst. Math. Appl.*, vol. 10, pp. 266–271, 1974.
- [27] R. Ammann, B. Grünbaum, and G. C. Shephard, “Aperiodic tiles,” *Discrete Comput. Geom.*, vol. 8, no. 1, pp. 1–25, 1992.

- [28] S. J. Ahn, P. Moon, T.-H. Kim, H.-W. Kim, H.-C. Shin, E. H. Kim, H. W. Cha, S.-J. Kahng, P. Kim, M. Koshino, *et al.*, “Dirac electrons in a dodecagonal graphene quasicrystal,” *Science*, vol. 361, no. 6404, pp. 782–786, 2018.
- [29] Z. You and S. Pellegrino, “Foldable bar structures,” *Int. J. Solids Struct.*, vol. 34, no. 15, pp. 1825–1847, 1997.
- [30] J. Patel and G. K. Ananthasuresh, “A kinematic theory for radially foldable planar linkages,” *Int. J. Solids Struct.*, vol. 44, no. 18-19, pp. 6279–6298, 2007.
- [31] G. Kiper, E. Söylemez, and A. Ö. Kişisel, “A family of deployable polygons and polyhedra,” *Mech. Mach. Theory*, vol. 43, no. 5, pp. 627–640, 2008.
- [32] L. Cabras and M. Brun, “Auxetic two-dimensional lattices with poisson’s ratio arbitrarily close to  $-1$ ,” *Proc. R. Soc. A*, vol. 470, no. 2172, p. 20140538, 2014.
- [33] W. T. Tutte, “A theorem on planar graphs,” *T. Amer. Math. Soc.*, vol. 82, no. 1, pp. 99–116, 1956.
- [34] S. Guest, “The stiffness of prestressed frameworks: a unifying approach,” *Int. J. Solids Struct.*, vol. 43, no. 3–4, pp. 842–854, 2006.

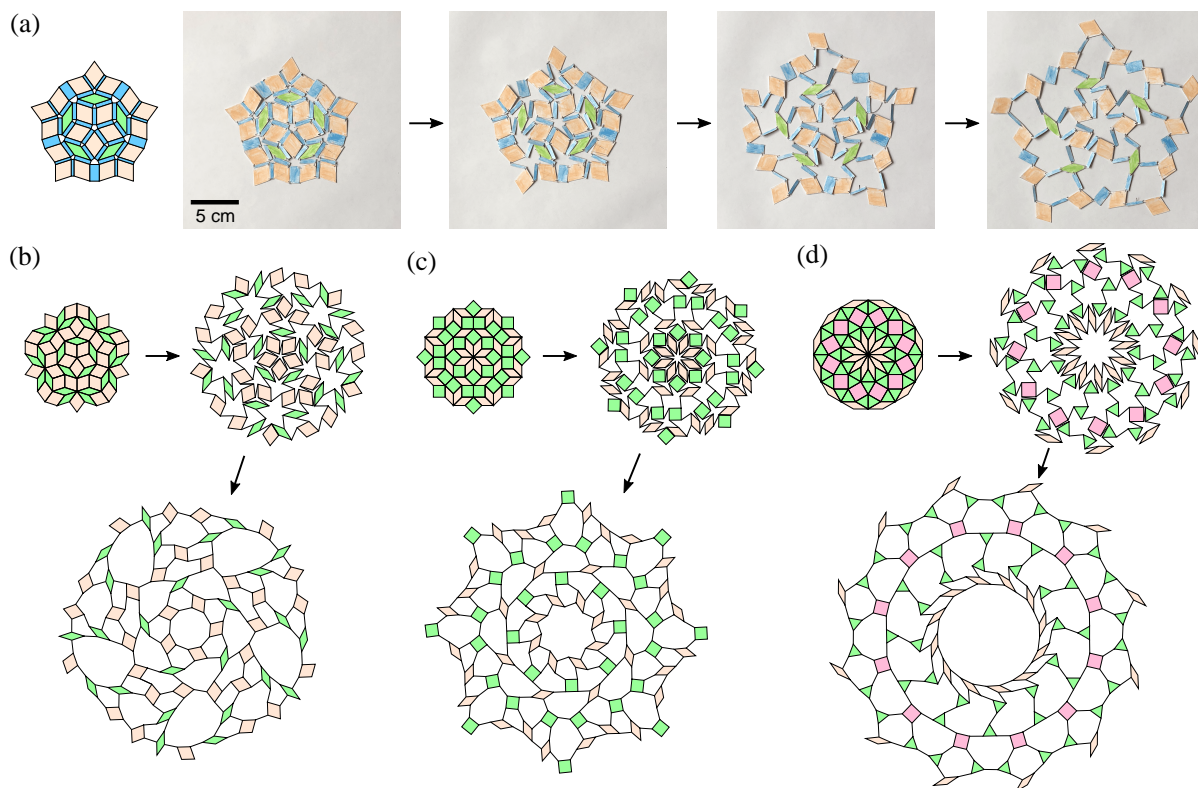


**Figure 1: Deployable quasicrystal patterns created using the expansion tile method.** (a) An example of the symmetry-preserving expansion method applied to the Penrose tiling and the deployment snapshots of a rigid cardstock paper model. (b) A deployable 5-fold Penrose tiling with ideal expansion tiles. (c) A deployable 8-fold Ammann–Beenker tiling with ideal expansion tiles. (d) A deployable 12-fold Stampfli tiling with ideal expansion tiles. For each example, the contracted state, an intermediate deployed state and the fully deployed state are shown.

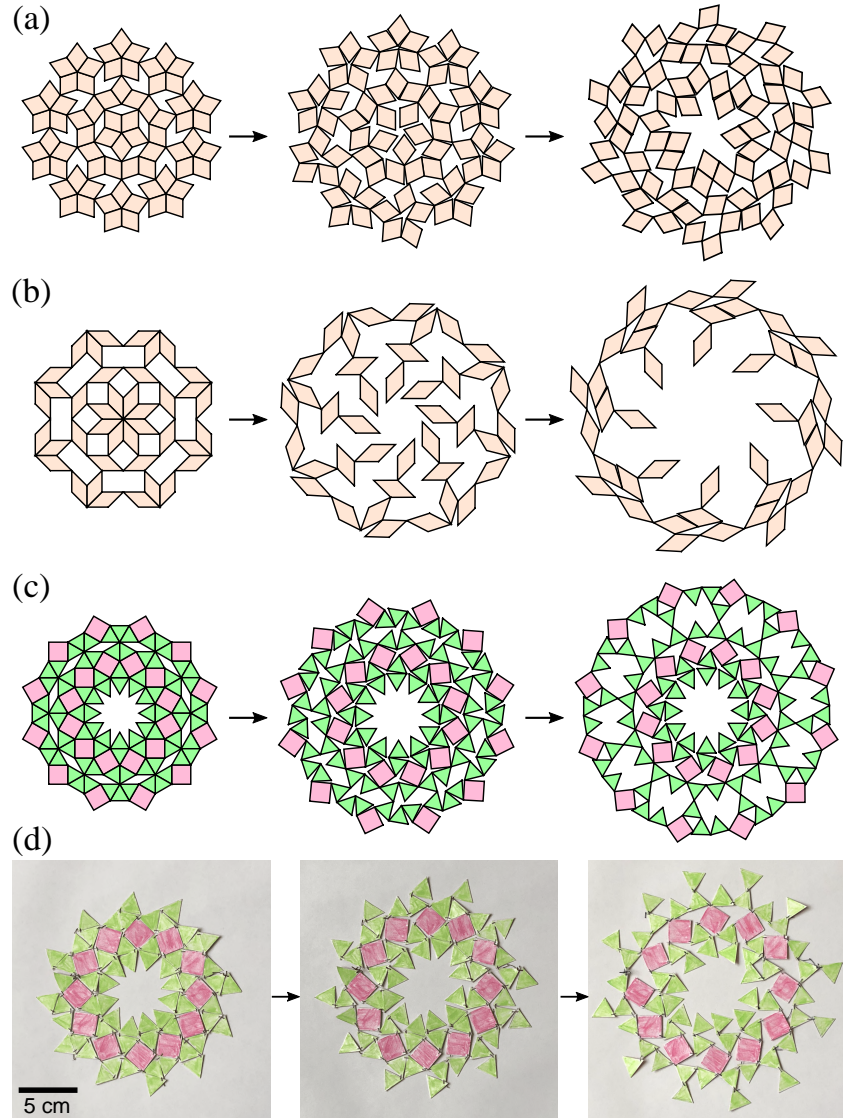
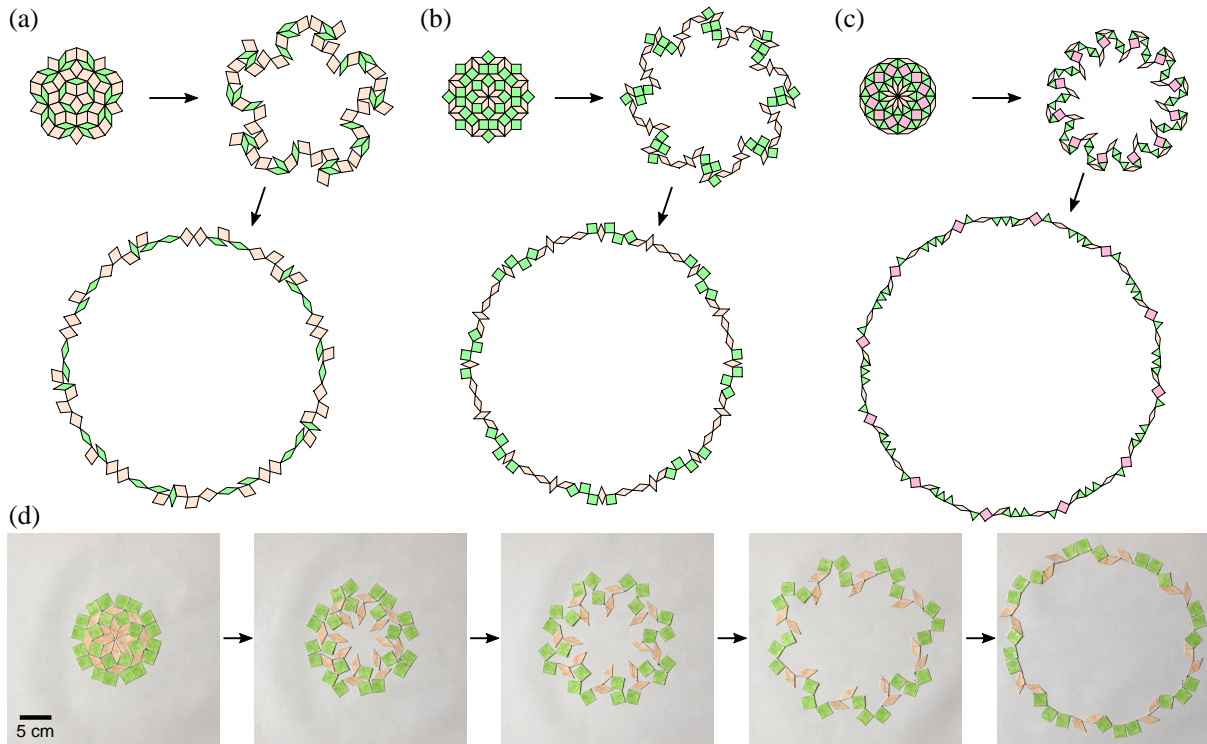


Figure 2: **Deployable quasicrystal patterns created using the tile removal method.** By removing certain tiles in a given quasicrystal pattern, we create holes and hence allow the pattern to be deployed. (a) A deployable 5-fold Penrose tiling. (b) A deployable 8-fold Ammann–Beenker tiling. (c) A deployable 12-fold Stampfli tiling. For each example, the contracted state, an intermediate deployed state and the fully deployed state are shown. (d) The deployment snapshots of a rigid cardstock paper model of a deployable Stampfli pattern.



**Figure 3: Deployable quasicrystal patterns created using the Hamiltonian cycle method.** We start by constructing a planar subgraph of the connectivity graph of the given quasicrystal pattern. We can then find a Hamiltonian cycle in the planar subgraph, which passes through all tiles exactly once and gives us a deployable structure. (a) A deployable 5-fold Penrose tiling. (b) A deployable 8-fold Ammann–Beenker tiling. (c) A deployable 12-fold Stampfli tiling. For each example, the contracted state, an intermediate deployed state and the fully deployed state are shown. (d) The deployment snapshots of a rigid cardstock paper model of a deployable Ammann–Beenker pattern.